JOURNAL OF MATERIALS SCIENCE 31 (1996) 2693–2696

Determination of the range of lattice distortion in AlN sintered body by higher order laue zone pattern

S. NAKAHATA, T. MATSUURA, K. SOGABE, A. YAMAKAWA
Itami Research Laboratories Sumitomo Electric Industries, Ltd.

To analyse the magnitude and range of lattice distortion which is responsible for the low thermal conductivity in aluminium nitride (AlN) crystal grains, the higher order laue zone (HOLZ) pattern of transmission electron microscopy was used. The HOLZ patterns obtained from various positions in the AlN crystal grain show that the AlN crystal lattice is distorted in the vicinity of the grain-boundary phase, and the magnitude of lattice distortion becomes large as it approaches the grain-boundary phase. Also, the range of distortion extends to approximately 300 nm from the grain-boundary phase.

1. Introduction

The high thermal conductivity and high ohmic resistance of aluminium nitride (AlN: wurtzite structure) make it a candidate as substrate material for integrated circuits. Slack [1] predicted the theoretical thermal conductivity to be 319 $W m^{-1} K$ at room temperature as a result of measurement of its values of AlN single crystals. On the other hand, polycrystalline AlN ceramics have various values from 100 $W m^{-1} K$ to 270 $W m^{-1} K$ since various kinds of defects such as grain-boundary, grain-boundary phase and impurities in the AlN crystal grains are included in polycrystalline AlN ceramics. These defects have been studied by many analytical methods [2–6]. One significant defect is lattice distortion in the AlN crystal grain. AlN crystal propagates heat by lattice waves. Therefore, the lattice distortion must be responsible for low thermal conductivity. The lattice distortions in the AlN crystal grain, however, have not been investigated.

In the measurement technique of lattice distortion, X-ray diffraction (XRD) is useful [7, 8]. However, XRD can only estimate an average value of one sample and cannot specify the position of lattice distortion. Observation with high resolution transmission electron microscopy provides direct information about atom location. However, if one were to try to obtain an absolute value of lattice distortion, a complicated dynamic simulation is necessary.

The higher order laue zone (HOLZ) pattern [9–11] which appeared in the bright field disc of the convergent beam electron diffraction pattern in transmission electron microscopy (TEM) is very sensitive to lattice shifts, and shows crystallographic information such as crystal symmetry, lattice distortion and lattice parameter in the local region a little less than 50 nm diameter. The HOLZ patterns are influenced by the dynamic effect, however, Tomokiyo [12] indicated that the HOLZ pattern can estimate an accurate absolute lattice parameter and magnitude of lattice distortion in kinematic approximation analysis if a suitable effective voltage (E_e) is chosen instead of the actual accelerating voltage. Therefore, analysis of HOLZ patterns and image observation are suitable techniques for the quantitative detection of the magnitude and region of local lattice distortions.

In this study, the magnitude and region of local lattice distortion in the AlN sintered body are described quantitatively by observation and analysis of the HOLZ patterns.

2. Experimental procedure

A commercial AlN powder, in which oxygen impurity was 0.98 wt % and the specific surface area was 3.3 $m^2 g^{-1}$, was mixed with 1.0 wt % of Y_2O_3 as a sintering aid and 2 wt % of thermoplastic organic binder in alcohol and moulded to a pellet shape. The green body was heated at 600 °C in a nitrogen atmosphere to remove binder. Sintering was carried out in a nitrogen atmosphere at 1850 °C for 3 h using a graphite furnace.

The density of the obtained sample was measured by Archimedes' method. The thermal conductivity of the sample was measured by the laser flash method at room temperature after the sample was processed to 10 mm diameter and 3 mm thickness and coated with carbonate. To estimate the composition of the sample, the XRD pattern was obtained in the range of $2\theta = 20$ to 80° using a copper target (CuK_α).

A foil specimen for the TEM observation was prepared by argon ion milling after cutting the sample and dimple grinding to about 20 μm thickness. The transmission electron microscope used was a Jeol JEM-2000FX, which is installed at the Research Laboratory of High Voltage Electron Microscope at Kyushu University. The TEM observations were performed at room temperature and operating voltage was set at 200 kV. The diameter of the electron probe

0022–2461

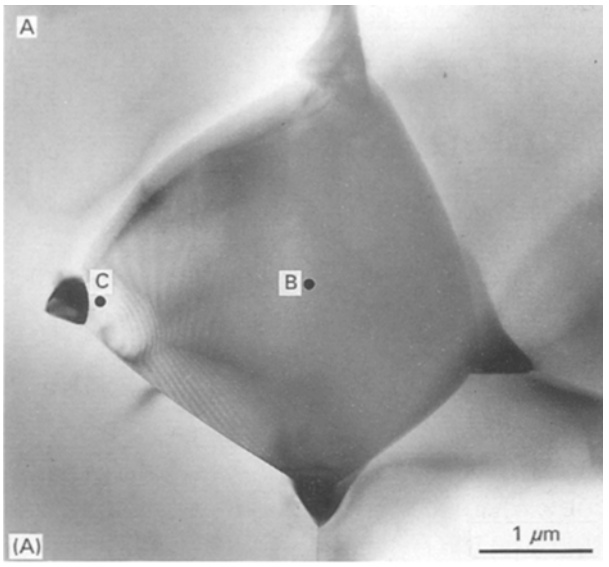

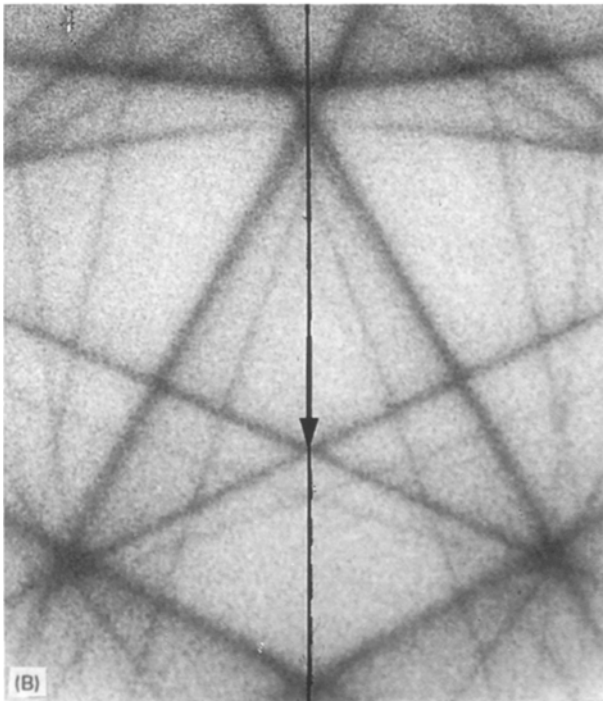

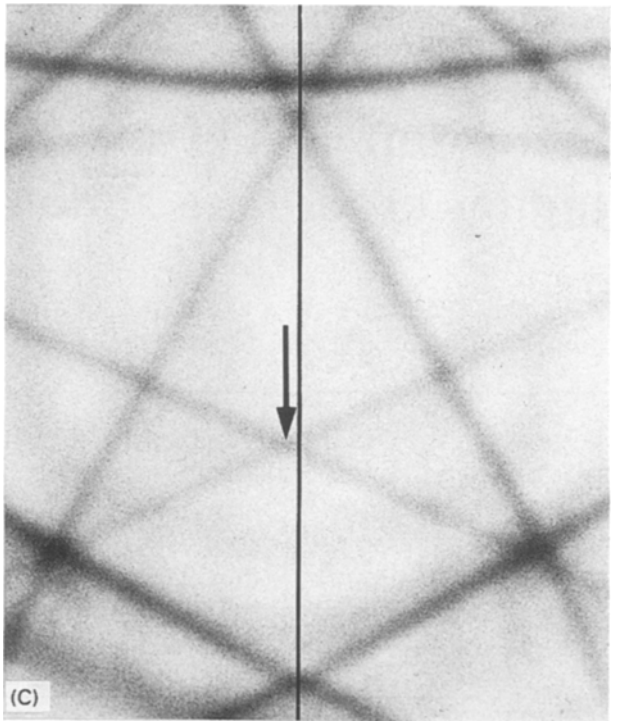

Figure 1 Bright field image of AlN sintered body (A) and HOLZ patterns (B) and (C) obtained from various positions shown in (A). Note the change of cross point position indicated by the arrow.

was less than about 20 nm. The specimen was oriented near to the [3 − 3 0 1] zone axis. To detect the lattice distortion, HOLZ patterns were obtained from various positions in AlN crystal grains. The obtained HOLZ patterns were analysed by kinematical approximation [11, 12] and the magnitudes of the lattice distortions were estimated.

3. Results and discussion

3.1. Detection of the local lattice distortion

The relative density of the sample is up to 99.9% and the thermal conductivity is 165 $W m^{-1} K$.

Fig. 1(A) shows a bright field image of the sample and the diameter of AlN crystal grains is approximately 5 μm. Fig. 1(B) and (C) show HOLZ patterns obtained from the centre of an AlN crystal grain and the AlN/grain-boundary phase shown in Fig. 1(A), respectively. One can see that Fig. 1(B) has symmetry to the solid line; however, Fig. 1(C) obtained from near the grain-boundary phase has lost its symmetry.

Fig. 2(A) shows a bright field image which is enlarged part of the grain-boundary phase shown in Fig. 1(A) and Fig. 2(B), (C), (D) and (E) show HOLZ patterns obtained from the various positions (B) to (E) as shown in the bright field image. Obtained HOLZ lines broaden as observed positions approach the grain-boundary phase. This result indicates that the arrangement of aluminium and nitrogen atoms in the AlN crystal lattice are disorderly and electron reflection is disturbed. The cross points indicated by the arrows in the HOLZ patterns, leave the symmetric position as the observed positions approach the grain-boundary phase. It is suggested that the magnitude of lattice distortion increases as approaching the grain-boundary phase.

3.2. Quantitative analysis

In order to measure the magnitude of lattice distortion from HOLZ patterns in kinematical approximation, a suitable E_e is estimated at $E_e = 199.6$ kV.

Fig. 3(a) and (b) show simulated HOLZ patterns using lattice constants $a = b = 0.3111$ nm ($a/b = 1$), $c = 0.4980$ nm, and $a = 0.3145$ nm, $b = 0.3111$ nm ($a/b = 0.995$), $c = 0.4980$ nm, respectively. It is apparent that if lattice constants a and b are not equal, the HOLZ pattern does not have symmetry to the dotted line shown in Fig. 3(b). It is suggested that the AlN crystal lattice near the grain-boundary phase is distorted and does not have a wurtzite structure.

For measurement of the magnitude of lattice distortion, the ratio of A/B, shown in Fig. 3(a), is adopted since A/B is very sensitive to the change of lattice ratio,

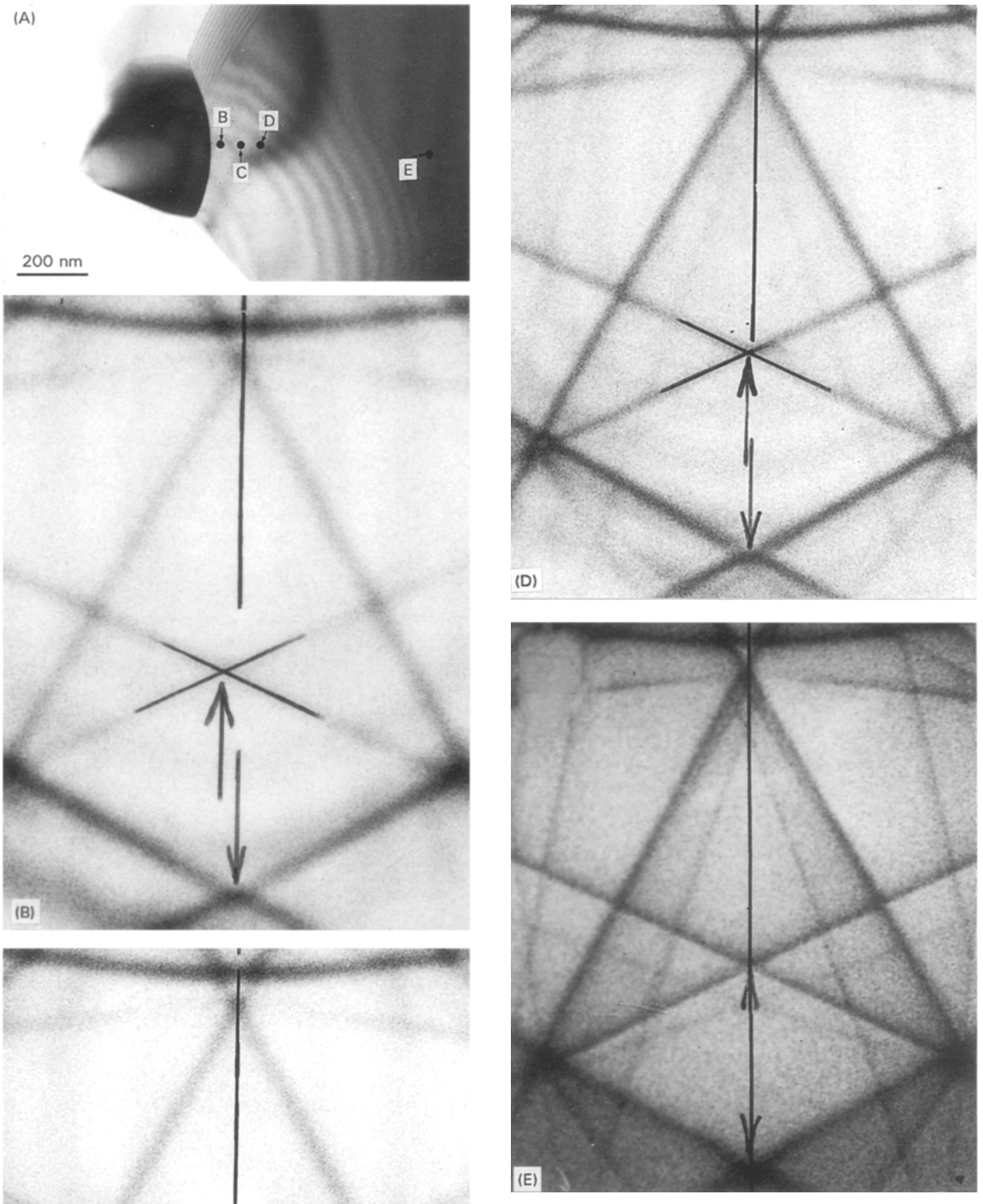

Figure 2 Bright field image of AlN sintered body (A) and HOLZ patterns (B) and (C) obtained from various positions shown in (A). Note the change of cross point position indicated by the arrow.

a/b. Fig. 4 shows the change of a/b as a function of A/B. One can understand that if the measurement error of A/B is large, the error of a/b becomes very small. For example, if the measured value of A/B is 1.15 ± 0.03, that is, measurement error is 2.6%, the value of a/b is estimated at 0.995 ± 0.001 and measurement error is just 0.1% as shown in Fig. 4.

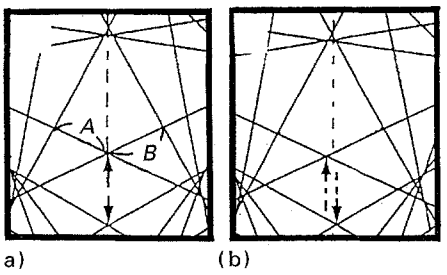

Figure 3 Simulated HOLZ pattern using lattice constants $a = b = 0.3111$ nm ($a/b = 1$), $c = 0.4980$ nm (a) and $a = 0.3145$ nm, $b = 0.3111$ nm ($a/b = 0.995$), $c = 0.4980$ nm (b).

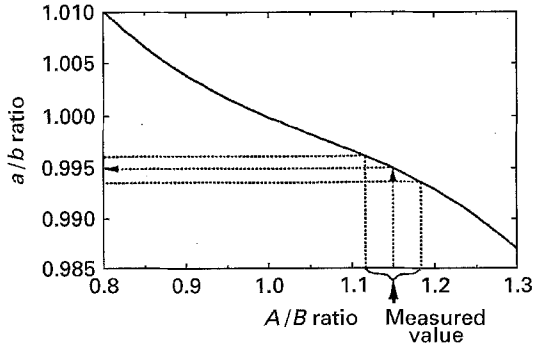

Figure 4 The a/b ratio as a function of A/B estimated from simulated HOLZ patterns.

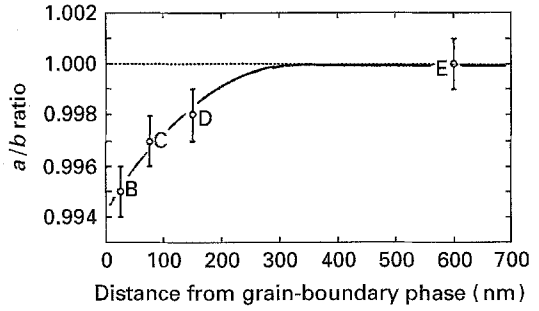

Figure 5 The a/b ratio as a function of the distance from the grain-boundary phase.

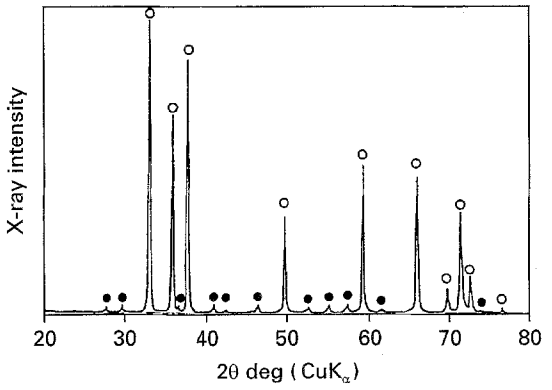

Figure 6 XRD pattern obtained from the AlN sintered body. ○ AlN, ● $3Y_2O_3 \cdot 5Al_2O_3$.

The value of a/b of the AlN crystal lattice shown in Fig. 2(B), (C), (D) and (E) is estimated using Fig. 4. Fig. 5 shows the a/b ratio as a function of the distance from the grain-boundary phase. This result indicates that the magnitude of lattice distortion in the AlN crystal grain becomes small as it parts from the grain-boundary phase and the lattice distortion is spread about 300 nm from the grain-boundary phase.

This lattice distortion is influenced by the difference of the thermal expansion coefficient between the AlN and the grain-boundary phase. The XRD study shows the composition of the grain-boundary phase is $3Y_2O_3 \cdot 5Al_2O_3$ shown in Fig. 6. The thermal expansion coefficient of AlN and $3Y_2O_3 \cdot 5Al_2O_3$ are 4.19×10^{-6} [13] and 6.96×10^{-6} [14], respectively. Therefore, lattice distortion is due to the difference of the thermal expansion coefficient.

4. Conclusion

The magnitude of the lattice distortion in AlN crystal grain has been investigated by HOLZ pattern analysis. The AlN–1.5 wt % $3Y_2O_3$ system was sintered. The HOLZ patterns obtained from various positions in the AlN crystal grain show that the AlN crystal is distorted in the vicinity of the grain-boundary phase and its region of the lattice distortion is estimated about 300 nm from the grain-boundary phase.

Acknowledgements

The authors wish to express gratitude to Professor Tomokiyo of HVEM Laboratories, Kyushu University, for his support and advice during observations using the Jeol 2000-FX analytical TEM, Mr Tanaka and Mr Manabe also of HVEM Laboratories who assisted in the operation of the microscope, and Mr Maekawa of Sumitomo Electric Industries who helped to prepare the AlN sintered body.

References

1. G. A. SLACK, *J. Phys. Chem. Solids.* **34** (1973) 321.
2. G. E. ARCHANGELSKII, M. V. FOCK, S. I. PACESOVA and L. JASTRABIK, *Phys. Stat. Sol. B* **108** (1981) K117.
3. R. A. YOUNGMAN and J. H. HARRIS, *J. Amer. Ceram. Soc.* **73** (1990) 3238.
4. G. E. POTTER, A. K. KNUDSEN, J. C. TOU and A. CHOUDHURY, *ibid.* **75** (1992) 3215.
5. L. E. McNEIL, M. GRIMSDITCH and R. H. FRENCH, *ibid.* **76** (1993) 1132.
6. M. STERNITZKE and G. MULLER, *ibid.* **77** (1994) 737.
7. C. J. N. WAGNER and E. N. AQUA, "Advances in X-ray analysis", Vol. 7 (Plenum Press, New York, 1964) p. 46.
8. E. N. AQUA and C. N. J. WAGNER, *Phil. Mag.* **9** (1964) 565.
9. J. A. EADES (ed.), Special issues of *J. Electron Microsc. Tech.* on "Convergent beam electron diffraction", **13** Nos. 1, 2 (1989).
10. M. J. KAUFMAN, D. D. PEARSON and H. L. FRASER, *Phil. Mag.* **A54** (1986) 79.
11. M. TANAKA, M. TERAUCHI and T. KANEYAMA, "Convergent beam electron diffraction" (Tokyo, Jeol-Maruzen, 1988).
12. Y. TOMOKIYO, S. MATSUMURA, N. KUWANO, M. KOMINAMI, T. OKUYAMA and K. OKI, *J. Electron Microsc.* **35** (1986) 359.
13. W. WERDECKER and F. ALDINGER, *IEEE Trans. Components, Hybrids, Manuf. Technol.* **CHMT-7** (1984) 399.
14. D. D. YOUNG, K. C. JUNGLING, T. L. WILLIAMSON and E. R. NICHOLS, *IEEE J. Quantum Elec.* **Aug.** (1972) 720.

Received 2 August 1994
and accepted 20 November 1995